THE JOURNAL OF PHYSICAL CHEMISTRY B
A JOURNAL OF THE AMERICAN CHEMICAL SOCIETY

pubs.acs.org/JPCB

Article

Beyond "Mega": Origin of the "Giga" Stokes Shift for Triazolopyridiniums

Adam N. Petrucci, Morgan E. Cousins, and Matthew D. Liptak*

Cite This: *J. Phys. Chem. B* 2022, 126, 6997−7005

Read Online

ACCESS | Metrics & More | Article Recommendations | Supporting Information

ABSTRACT: Over the past decade, fluorophores that exhibit "mega" Stokes shifts, defined to be Stokes shifts of greater than 100 nm, have gained considerable attention due to their potential technological applications. A subset of these fluorophores have Stokes shifts of at least 10,000 cm^{-1}, for whom we suggest the moniker "giga" Stokes shift. The majority of "giga" Stokes shifts reported in the literature arise from the twisted intramolecular charge transfer mechanism, but this mechanism does not fit empirical characterization of triazolopyridinium (TOP). This observation inspired a density functional theory (DFT) and time-dependent DFT study of TOP, and several related fluorophores, to elucidate the novel photophysical origin for the "giga" Stokes shift of TOP. The resulting computational models revealed that photoexcitation of TOP yields a zwitterionic excited state that undergoes significant structural relaxation prior to emission. Most notably, TOP has two orthogonal moieties in the ground state that adopt a coplanar geometry in the excited state. According to Hückel's rule, both the heterocycle and phenyl moieties of TOP should be aromatic in an orthogonal ground state. However, according to Baird's rule, these individual moieties should be anti-aromatic in the excited state. By relaxing to a coplanar conformation in the excited state, TOP likely forms a single aromatic system consisting of both the heterocycle and phenyl moieties.

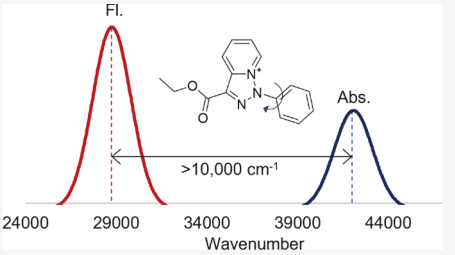

INTRODUCTION

The development of organic fluorophores with large Stokes shifts is a growing area of scientific research with tremendous technological potential. The moniker "mega" Stokes shift was first used in 2010 to describe fluorophores with Stokes shifts of greater than 100 nm,[1] and the set of molecules that fit this criterion has recently been reviewed.[2] However, this definition of a large Stokes shift is somewhat misleading. In general, the large energy difference between the absorption and emission bands of "mega" Stokes shift fluorophores minimizes self-absorption and favors technological applications. Thus, a major motivation for identifying new "mega" Stokes shift fluorophores is to minimize the overlap between the excitation and emission bands. The overlap of the excitation and emission bands depends upon both the Stokes shift and the bandwidths, so the role of bandwidths also needs to be considered. In solution, the main contribution to emission and excitation bandwidths is an unresolved vibronic structure. As a result, bandwidths are relatively consistent for aromatic molecules when quantified in an energy unit such as wavenumbers. However, when bandwidths are reported in wavelength, near-infrared (nIR) bands are significantly broader than ultraviolet (UV) bands due to the nonlinear dependence of energy on wavelength in the Planck−Einstein relation. Consequently, it can be difficult to distinguish fluorophores with minimal overlap between their excitation and emission bands from fluorophores with moderate overlap that emit in the nIR when quantifying the Stokes shift in wavelength. This issue can be avoided by reporting Stokes shifts in energy units, such as wavenumbers.

Compared to "mega" Stokes shift fluorophores,[1,2] a much smaller set of molecules have Stokes shifts greater than 10,000 cm^{-1},[3−7] for whom we suggest the designation "giga" Stokes shift. In the past, "mega" Stokes shift fluorophores have been utilized for imaging,[1,8−13] thermometry,[4,14] sensing,[15−17] and organic light-emitting diode (OLED)[18] applications. Several of these applications rely upon the minimal self-absorption of "mega" Stokes shift fluorophores, which is expected to be further minimized for "giga" Stokes shift fluorophores. Thus, the preparation of novel organic fluorophores that exhibit "giga" Stokes shifts is expected to be of considerable technological utility.

To date, "giga" Stokes shifts have been attributed to the twisted intramolecular charge transfer (TICT) mechanism. TICT is a phenomenon whereby two coplanar moieties adopt a perpendicular orientation in the electronic excited state to decouple the cationic and anionic radicals generated by charge transfer.[19] The photophysics of a number of "giga" Stokes shift fluorophores have been attributed to the TICT mechanism

Received: June 24, 2022
Revised: August 10, 2022
Published: September 5, 2022

https://doi.org/10.1021/acs.jpcb.2c04397
J. Phys. Chem. B 2022, 126, 6997−7005

based upon time-dependent density functional theory (TDDFT) calculations.[4−6] One major contribution to the Stokes shift of TICT fluorophores is excited structural relaxation. The zwitterionic excited state is stabilized by a twisted geometry, whereas the neutral ground state is destabilized by a twisted geometry, resulting in a smaller energy gap and red-shifted emission compared to the excitation wavelength. A second major contribution to the Stokes shift of TICT fluorophores is the influence of the zwitterionic excited state on the solvent structure. The zwitterionic excited state will induce a significant reorganization of the solvent structure, particularly for a polar solvent. Again, this will stabilize the excited state, destabilize the ground state, and red-shift the emission transition relative to the excitation transition.

The noteworthy exception to the emerging paradigm that "giga" Stokes shifts arise from TICT is triazolopyridinium (TOP). Efficient syntheses of TOP and the TOP dimer (TOP_2) using a Cu(II) oxidant were first reported in 2013 (Figure 1).[3] TOP exhibited a "giga" Stokes shift of 11,790

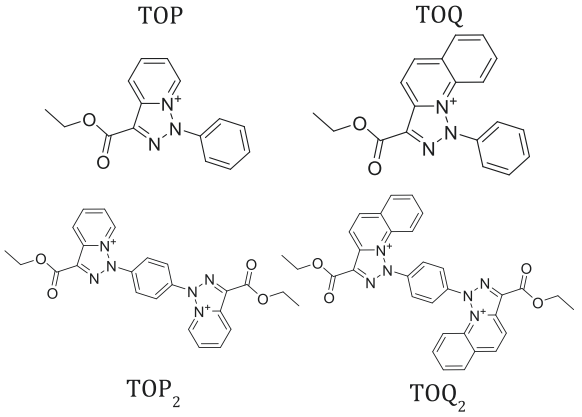

Figure 1. Fluorophores whose photophysical mechanisms were modeled in this article. These include monomeric and dimeric triazolopyridiniums (TOP and TOP_2), plus monomeric and dimeric triazoloquinoliniums (TOQ and TOQ_2).

cm^{-1} in water, and the excitation transition was assigned to intramolecular charge transfer based upon TDDFT calculations. Later, in 2017, efficient syntheses of the triazoloquinolinium monomer (TOQ) and triazoloquinolinium dimer (TOQ_2) were reported, along with more extensive characterization of the photophysics for this family of dyes.[7] Importantly, X-ray crystallographic characterization of TOP, and computational modeling of TOQ, has indicated that these molecules adopt twisted ground-state geometries. Thus, the "giga" Stokes shifts of TOP cannot arise from TICT because it is already twisted prior to photoexcitation. This observation motivated us to launch a detailed investigation of the photophysical mechanisms for TOP and TOQ dyes to gain insight into an alternative strategy for preparing "giga" Stokes shift fluorophores.

In this work, spectroscopically validated density functional theory models for triazolopyridinium and triazoloquinolinium salts were developed to gain insight into the novel photophysics of the "giga" Stokes shift fluorophores. Ground-state (S_0) geometries for TOP, TOP_2, TOQ, and TOQ_2 were predicted using six different density functionals. The DFT-predicted S_0 geometries for TOP were compared to the X-ray crystal structure of this molecule to assess the accuracies of ground-state structures predicted by each functional.[3] Next, the excitation spectra for all four dyes were modeled by TDDFT calculations using the same six functionals. The accuracies of these predictions were gauged by comparing the experimental and TDDFT-predicted UV/Vis absorption (Abs) spectra.[3,7] Finally, TDDFT was employed to predict the excited-state (S_1) geometries and emission spectra for TOP, TOP_2, TOQ, and TOQ_2. The experimental and predicted Stokes shifts were compared to judge the accuracy of these calculations. Ultimately, these models revealed that the "giga" Stokes shift of TOP arises from a photophysical mechanism that can be rationalized with Hückel and Baird's rules.[20−23]

METHODS

Ground-State Electronic Structure Calculations. The minimum energy ground-state geometries of all four dyes were obtained via complete geometry optimization calculations using DFT. The initial structural model of TOP was based upon the X-ray crystal structure of this molecule.[3] Initial structural models for TOP_2, TOQ, and TOQ_2 were prepared by modifying the TOP starting structure using the Argus Lab software program (Planaria software). All electronic structure calculations reported in this article utilized the ORCA 4.0.0.2 software program as installed on the Vermont Advanced Computing Core.[24] Geometry optimizations were conducted using the BLYP,[25,26] PBE,[27] B3LYP,[28] PBE0,[29] ωB97,[30] and ωB97X[30] density functionals. All geometry optimizations utilized a def2-TZVP basis set,[31] a def2/J auxiliary basis set,[32] and the TightSCF convergence algorithm. For the hybrid density functionals, the RIJCOSX method was used to speed up calculation of the Coulomb and exchange terms.[33] Cartesian coordinates for all fully optimized gas phase structures are available in the Supporting Information.

Following complete geometry optimization in the gas phase, the electronic structures of each dye were calculated in solution. Single-point calculations were completed using the same density functionals and basis sets noted above with the addition of a conductor-like polarizable continuum model (CPCM) for solvent.[34] For TOP and TOP_2, the CPCM parameters were set to model solvation by water. For TOQ and TOQ_2, the CPCM parameters were set to model solvation by methanol and acetonitrile, respectively. To aid in the analysis of the DFT data, valence molecular orbitals (MOs) were plotted in gOpenMol with isodensity values of 0.001 a.u.[35,36]

Excited-State Electronic Structure Calculations. The UV/Vis Abs spectra of the four dyes were predicted using TDDFT calculations. All UV/Vis Abs spectral prediction calculations utilized the fully optimized, gas phase geometries. These calculations employed the same density functionals, basis sets, and solvation models as the ground-state calculations. To predict the UV/Vis Abs spectra, the 20 lowest energy excited states were predicted using TDDFT with an expansion space of 120 vectors. The predicted UV/Vis Abs spectra shown in this article were generated by convoluting Gaussian-shaped bands with full-width, half-maximum bandwidths of 2500 cm^{-1}.

The Stokes shifts for each dye were predicted using excited-state geometry optimizations. The starting structures for these calculations were the fully optimized, ground-state structures. Excited-state geometry optimization calculations employed the same density functionals and basis sets noted above but did not

https://doi.org/10.1021/acs.jpcb.2c04397
J. Phys. Chem. B 2022, 126, 6997−7005

include an implicit solvent model. TDDFT, using the same parameters as for the UV/Vis Abs spectral predictions, was used to calculate the minimum energy structure for the S_1 excited state of each dye. Cartesian coordinates for all S_1 excited-state structures are available in the Supporting Information.

Finally, the fluorescence spectra for all four solvated dyes were predicted using CPCM and TDDFT. All fluorescence spectral predictions employed the S_1 excited-state geometries. The fluorescence spectral predictions employed the same density functionals, basis sets, and solvation models described above. The TDDFT calculations used the same parameters as for the UV/Vis Abs spectral predictions. Again, to aid in the analysis of the DFT data, valence MOs were plotted in gOpenMol with isodensity values of 0.001 a.u.[35,36] Finally, the fluorescence spectra were generated by convoluting Gaussian-shaped bands with full-width, half-maximum bandwidths of 2500 cm^{-1}.

RESULTS

S_0 Ground-State Geometries. The S_0 ground-state geometry of TOP was predicted using a variety of density functionals and compared to published X-ray crystal structure data. Structural models were prepared based upon generalized gradient approximation (GGA) functionals (BLYP and PBE),[25−27] hybrid functionals (B3LYP and PBE0),[28,29] and range-separated functionals (ωB97 and ωB97X).[30] All structural models utilized a def2-TZVP triple-ζ basis set.[31] Generally, all six density functionals provided good models for the TOP structure, with RMSD values between the computational and crystallographic structures ranging from 0.253 to 0.354 Å for the nonhydrogen atoms (Figure 2 and Figures S1−S5).[3] The B3LYP model had the smallest RMSD of all six, so this model was used for all further ground-state structural analysis. It is important to note that, in addition to a good overall RMSD, all DFT-predicted N−N bond lengths within the triazole moiety, and the C−N bond length between the heterocycle and phenyl moieties, were in excellent agreement with experiment (Table 1 and Tables S1−S5). Thus, although the B3LYP density functional yielded the most accurate structural model for TOP, all six density functionals predicted S_0 geometries in good agreement with experiment.

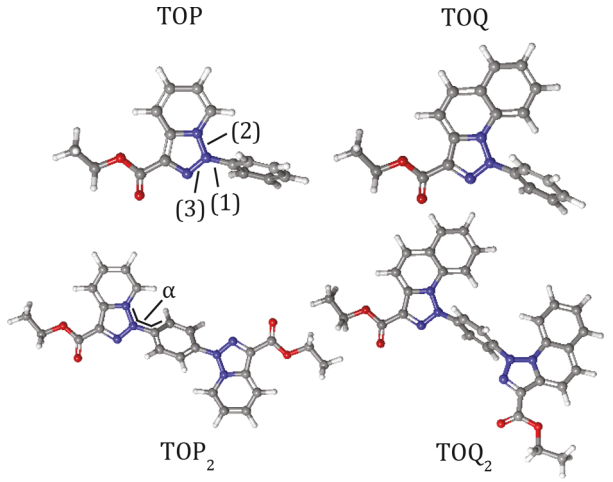

Figure 2. S_0 ground-state geometries of TOP (top left), TOP_2 (bottom left), TOQ (top right), and TOQ_2 (bottom right). The ground-state structures were optimized using the B3LYP density functional and the def2-TZVP basis set. The RMSD between B3LYP/def2-TZVP and the crystallographic structure of TOP is 0.253 Å for the nonhydrogen atoms.

Table 1. B3LYP S_0 Geometries of TOP Dyes

	1 (Å)[a]	2 (Å)[a]	3 (Å)[a]	α (°)[a]
TOP(exp)[b]	1.439	1.364	1.323	59.7
TOP(DFT)	1.436	1.368	1.311	66.7
TOP_2(DFT)[c]	1.426	1.370	1.320	55.6
TOQ(DFT)	1.442	1.375	1.311	51.0
TOQ_2(DFT)[c]	1.445	1.383	1.324	58.0

[a]See Figure 2. [b]Ref 3. [c]Data reported for TOP_2 and TOQ_2 are the average for both heterocycle moieties.

Next, the B3LYP density functional was used to predict the ground-state structures of TOP_2, TOQ, and TOQ_2. The lengths of three key bonds for the triazole moiety are relatively unperturbed by the substituent changes (Table 1). For all four dyes, the average C−N linker bond length is 1.44 Å, with a standard deviation of <0.01 Å, and all four dyes exhibit asymmetric bonding within the triazole moiety (average bond lengths of 1.37 and 1.32 Å, with standard deviations of <0.01 Å). All four dyes also exhibit rotation about the heterocycle−phenyl linker. The average rotation about the C−N linker bond is 60°, with a standard deviation of <10°, which should be sufficient to break the conjugation between the heterocycle and phenyl moieties. This bond rotation can be readily understood in terms of Hückel's rule, which states that conjugated π systems with $4n + 2$ electrons are aromatic, whereas conjugated π systems with $4n$ electrons are anti-aromatic.[20−22] The triazolopyridinium heterocycle contains 10 π electrons, the triazoloquinolinium heterocycle contains 14 π electrons, and the phenyl ring has six π electrons. Thus, each of these ring systems is expected to be aromatic, but the coplanarity of the heterocycle and phenyl rings would be expected to create an anti-aromatic system. In summary, the twisted S_0 ground-state geometries of TOP, TOP_2, TOQ, and TOQ_2 can all be rationalized on the basis of Hückel's rule.

UV/Vis Abs Spectra. The UV/Vis Abs spectra of all four TOP and TOQ dyes were predicted using TDDFT. Briefly, the electronic structures of solvated dyes were predicted using the optimized S_0 ground-state geometries described above, the same six density functionals described above, and the CPCM implicit solvation model.[34] TDDFT was employed to model the excited-state electronic structures and UV/Vis Abs spectra of these dyes (Figure 3 and Figures S6−S10). The GGA functionals consistently underestimated the electronic transition energies measured by UV/Vis Abs spectroscopy, whereas the hybrid and range-separated functionals consistently overestimated the electronic transition energies (Table 2). Overall, the B3LYP/def2-TZVP model yielded the most accurate transition energies with an average absolute error of 600 cm^{-1} between this model and experiment.

However, the TDDFT-predicted UV/Vis Abs intensities are a better gauge for the accuracy of these calculations than the TDDFT-predicted UV/Vis Abs energies. The trend observed above where the transition energies increase with increasing amounts of Hartree−Fock exchange had been observed previously for a set of 29 functionals and 500 molecules.[37] So, the accurate prediction of the transition energies by the B3LYP functional may simply arise from a cancellation of

https://doi.org/10.1021/acs.jpcb.2c04397
J. Phys. Chem. B 2022, 126, 6997−7005

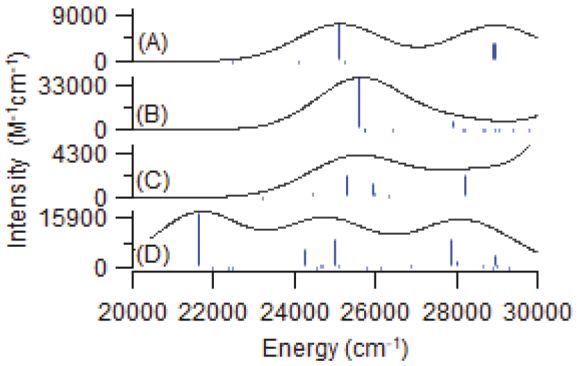

Figure 3. TDDFT-predicted UV/Vis Abs spectra for the TOP monomer in water (A), TOP dimer in water (B), TOQ monomer in methanol (C), and TOQ dimer in acetonitrile (D). The electronic structures were modeled using the BLYP density functional and the def2-TZVP basis set. The solvent was modeled using the CPCM implicit solvation model.

Table 2. $S_0 \rightarrow S_1$ Abs Energies (cm^{-1}) of TOP Dyes

	TOP	TOP_2	TOQ	TOQ_2	error
(exp)	33,100[a]	32,200[a]	29,300[b]	28,800[b]	
BLYP	25,100	25,700	25,600	21,700	6300
PBE	26,000	25,800	26,200	22,000	5900
B3LYP	33,600	31,800	30,200	29,400	600
PBE0	35,700	32,800	31,600	31,100	2000
ωB97	42,100	38,100	36,200	34,000	6800
ωB97X	41,800	38,500	35,800	35,400	7000

[a]Ref 3. [b]Ref 7.

errors derived from the overall biases of these functionals. Alternatively, the TDDFT-predicted UV/Vis Abs intensities depend upon the overlap between the donor and acceptor states. As a result, the TDDFT-predicted UV/Vis Abs intensities are excellent indicators for the accuracy of the valence orbital shapes predicted by DFT.

Based upon the observed and predicted UV/Vis intensities, the BLYP model provides the most accurate model for the valence electronic structures of TOP and TOQ dyes. The UV/Vis Abs intensities predicted by the GGA functionals are an order of magnitude more accurate than the intensities predicted by the hybrid and range-separated functionals (Table 3). Overall, the UV/Vis Abs intensities predicted by the BLYP functional are the most accurate with an average absolute error of 6500 M^{-1} cm^{-1}. Consequently, the BLYP functional is considered to provide the most accurate models for the excitation transitions and excitation band assignments made in this article will exclusively rely upon the BLYP model.

Table 3. $S_0 \rightarrow S_1$ Abs Intensities (M^{-1} cm^{-1}) of TOP Dyes

	TOP	TOP_2	TOQ	TOQ_2	error
(exp)	11,100[a]	22,100[a]	8100[b]	16,400[b]	
BLYP	7200	38,800	4100	17,800	6500
PBE	8900	46,100	6700	24,500	8900
B3LYP	20,600	70,600	17,100	25,000	18,900
PBE0	26,200	80,300	19,100	27,800	23,900
ωB97	17,400	84,100	23,000	56,300	30,800
ωB97X	17,200	74,100	23,500	41,500	24,700

[a]Ref 3. [b]Ref 7.

Excitation Transitions. The BLYP/def2-TZVP models for TOP and TOP_2 suggest charge transfer and $\pi \rightarrow \pi^*$ assignments, respectively. The electron density difference map (EDDM) for TOP, predicted using the BLYP density functional, illustrates that the excitation transition for this molecule partially transfers an electron from the phenyl moiety to the triazolopyridinium heterocycle (Figure 4). Some

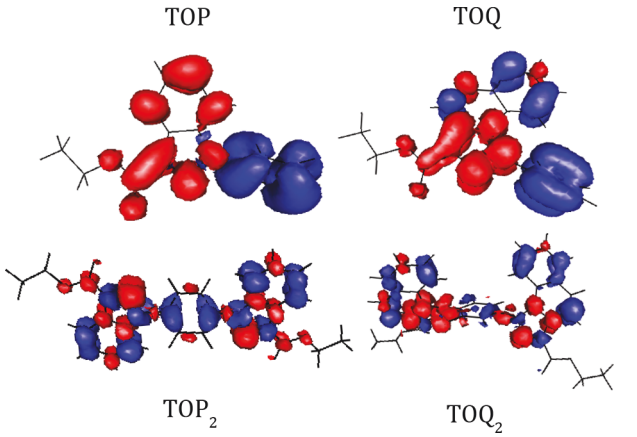

Figure 4. TDDFT-predicted UV/Vis Abs transitions for TOP in water (A), TOP_2 in water (B), TOQ in methanol (C), and TOQ_2 in acetonitrile (D). Blue indicates loss of electron density, and red indicates gain of electron density. The electronic structures were modeled using the BLYP density functional and the def2-TZVP basis set. The solvent was modeled using the CPCM implicit solvation model.

alternative band assignments are suggested by the other density functionals (Figures S11–S15), which emphasize the importance of using spectroscopically validated models for band assignments. Thus, the best assignment for the TOP excitation transition is phenyl → heterocycle charge transfer. In contrast, the EDDM for TOP_2 suggests that the electron donation and acceptance for the excitation transition are delocalized throughout the entire molecule. The best description for this electronic transition is a $\pi \rightarrow \pi^*$ transition. These spectral assignments are fully consistent with those made in an earlier work based upon a PBE model.[3] Also as noted previously, the addition of a second heterocyclic moiety to TOP fundamentally changes the nature of the excitation transition.

The TOQ and TOQ_2 excitations are also assigned to charge transfer and $\pi \rightarrow \pi^*$ transitions, respectively. Compared to TOP, there is additional electron donation from the heterocycle moiety in the TOQ excitation transition (Figure 4). However, this transition is still best described as a phenyl → heterocycle charge transfer since the phenyl moiety is primarily an electron donor. The excitation spectra of TOQ were previously modeled using semi-empirical calculations.[7] The band assignments made here based upon TDDFT are generally in agreement with this previous report. In addition, the TOP_2 and TOQ_2 transitions are quite similar. Both involve electron donation and electron acceptance throughout the entire molecule and are assigned to $\pi \rightarrow \pi^*$ transitions. Thus, the excitation transitions of TOP and TOQ can best be described as phenyl → heterocycle charge transfer transitions, whereas the excitation transitions of TOP_2 and TOQ_2 are better described as $\pi \rightarrow \pi^*$ transitions.

https://doi.org/10.1021/acs.jpcb.2c04397
J. Phys. Chem. B 2022, 126, 6997−7005

Stokes Shifts. A critical component of TOP and TOQ photophysics that had not been modeled prior to this work is the Stokes shift. The Stokes shift is the energy difference between the absorption and emission transitions observed using UV/Vis Abs and fluorescence spectroscopy, respectively. A Stokes shift is observed when the energy difference between the ground and excited electronic states differs for the ground- and excited-state geometries. One component of this energy change is intramolecular; electron excitation changes the bonding throughout a molecule, which alters the minimum energy structure. A second component of the Stokes shift is intermolecular; solvent molecules will rearrange to stabilize the altered charge distribution in the electronic excited state, which is particularly significant for charge transfer transitions. In this work, the intramolecular component has been modeled with excited-state geometry optimizations using TDDFT. The intermolecular component has been modeled by predicting the electronic transition energies for both the ground- and excited-state geometries following the addition of a CPCM implicit solvation model (Figure 5 and Figures S16–S20).[34]

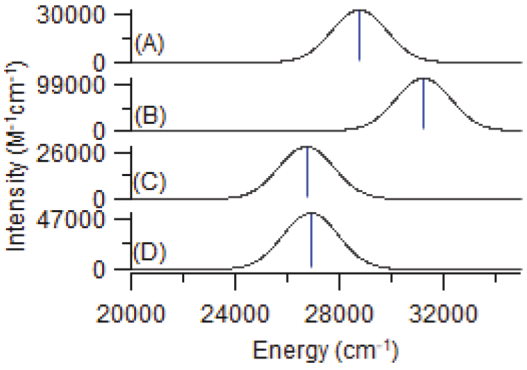

Figure 5. TDDFT-predicted fluorescence emission spectra for TOP in water (A), TOP_2 in water (B), TOQ in methanol (C), and TOQ_2 in acetonitrile (D). The electronic structures were modeled using the ωB97 density functional and the def2-TZVP basis set. The solvent was modeled using the CPCM implicit solvation model.

These considerations mean that the accuracy of the computed Stokes shift offers an assessment for the accuracies of the excited-state geometry optimization, the excitation transition, and the emission transition.

Overall, the range-separated hybrid functionals offer the best models for the Stokes shift of TOP and TOQ dyes. Although the GGA functionals do yield the most accurate model for the excitation transition of these molecules, the Stokes shifts predicted by these molecules have poor agreement with experiment (Table 4). Furthermore, the GGA functionals predict one or more dark states at energies lower than the emissive states noted in Table 4, suggesting that these dyes are quenched,[38] which is inconsistent with experimental data. The hybrid functionals do offer a moderate improvement over the GGA functionals with regard to the Stokes shift. B3LYP- and PBE0-predicted Stokes shifts have average absolute errors of 4900 and 4700 cm^{-1}, respectively, and there is only one instance where a dye is predicted to be quenched. However, the range-separated functionals clearly offer the most accurate models for the Stokes shift of TOP and TOQ dyes. The Stokes shifts predicted by the ωB97 and ωB97X functionals have average absolute errors of merely 900 and 1600 cm^{-1}, respectively, and all TOP and TOQ dyes are predicted to be emissive. It should be noted that the emission energies predicted by the ωB97 and ωB97X functionals are not particularly accurate due to the sizable errors in the excitation energy predictions (Table 2). However, the systematic overestimation of S_1 excited-state energies by these functionals cancels out when the differences between the excitation and emission energies are taken to calculate the Stokes shifts. Overall, the ωB97 functional offers the most balanced treatment for all the components of the Stokes shift.

Table 4. Stokes Shifts (cm^{-1}) for TOP Dyes

	TOP	TOP_2	TOQ	TOQ_2	error
(exp)	11,200[a]	7800[a]	9200[b]	7000[b]	
BLYP	10,200[c]	22,500[c]	13,100[c]	19,900[c]	8100
PBE	9400[c]	19,900[c]	13,600[c]	19,700[c]	7800
B3LYP	17,900	6600[c]	15,300	12,700	4900
PBE0	18,100	6100	14,800	11,700	4700
ωB97	13,300	6900	9500	7100	900
ωB97X	14,900	7900	9900	9000	1600

[a]Ref 3. [b]Ref 7. [c]Quenched.

Emission Transitions. In general, the ωB97/def2-TZVP models predict that the emission transitions for TOP and TOQ are the inverse of the excitation transitions. The EDDM for the TOP emission transition, predicted using the ωB97 density functional, illustrates that the fluorescence of this molecule arises from heterocycle → phenyl charge transfer (Figure 6). The charge transfer transition relieves the zwitterionic character of the excited state, resulting in a structurally perturbed version of the S_0 ground state. As is the case for the excitation transitions, there are differences between the emission transitions predicted by various density functionals (Figures S21–S25). However, the ωB97 data are presented here based upon the agreement between the experimental and computed Stokes shifts (Table 4). The EDDM for TOQ also suggests a heterocycle → phenyl charge transfer to relieve the zwitterionic character of the excited state. In both cases, the emission transitions are roughly the inverse

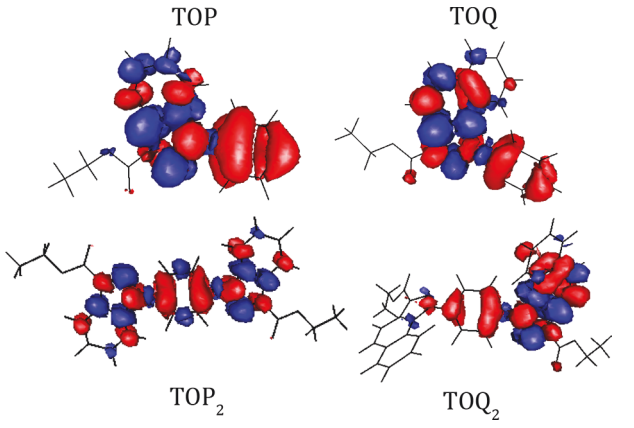

Figure 6. TDDFT-predicted fluorescence emission transitions for TOP in water (A), TOP_2 in water (B), TOQ in methanol (C), and TOQ_2 in acetonitrile (D). Blue indicates loss of electron density, and red indicates gain of electron density. The electronic structures were modeled using the ωB97 density functional and the def2-TZVP basis set. The solvent was modeled using the CPCM implicit solvation model.

https://doi.org/10.1021/acs.jpcb.2c04397
J. Phys. Chem. B 2022, 126, 6997–7005

of the excitation transitions (Figure 4). The small differences between the excitation and emission transitions can be attributed to vibronic relaxation in the S_1 excited state following excitation and prior to emission. Thus, for TOP and TOQ, structural relaxation in the electronic excited state does not fundamentally alter the electronic transition.

The photophysics of TOP_2 and TOQ_2 are more complicated than those of TOP and TOQ. The TOP_2 emission transition can be assigned to a $\pi^* \rightarrow \pi$ transition based upon the EDDM (Figure 6). Similar to the cases for TOP and TOQ, this is roughly the inverse of the excitation transition for this compound (Figure 4). On the other hand, the TOQ_2 emission transition is best described as a charge transfer from one of the heterocycle moieties to the phenyl linker. This transition is fundamentally different from the $\pi \rightarrow \pi^*$ excitation transition for this molecule and implies significant electronic reorganization during structural relaxation of the S_1 excited state for TOQ_2. The fundamental differences between the TOP_2 and TOQ_2 emission transitions predicted by TDDFT are supported by previously published quantum yield data.[7] The quantum yield of TOP_2 (0.22) is double that of TOQ_2 (0.11), which correlates with the larger TDDFT-predicted oscillator strength for the TOP_2 emission (1.29) compared to the TOQ_2 emission (0.60). The quantum yield of TOP_2 is significantly larger than the other three molecules in this study because it maintains a $\pi \rightarrow \pi^*$ excited state that has excellent overlap with the ground state following excited-state relaxation.

S_1 Excited-State Geometries. With spectroscopically validated models for the S_0 and S_1 structures available, it was possible to make comparisons to reveal the excited-state distortions. TOP and TOQ exhibit dramatic ring rotations in the S_1 excited states predicted by the ωB97 density functional (Figure 7). The dihedral angles between the heterocycle and

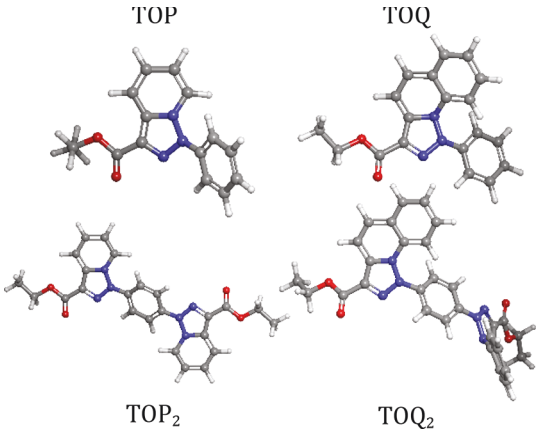

Figure 7. S_1 excited-state geometries of TOP (top left), TOP_2 (bottom left), TOQ (top right), and TOQ_2 (bottom right). The excited-state structures were optimized using the ωB97 density functional and the def2-TZVP basis set. Excitation to the S_1 excited state induces significant rotation about the heterocycle−phenyl bond.

phenyl moieties decrease to 6.4° and 3.0°, respectively, which are nearly coplanar (Table 5). Ring rotations are also observed in TOP_2 and TOQ_2, albeit to a lesser extent. The average heterocycle−phenyl dihedrals in TOP_2 and TOQ_2 are 25.9° and 18.1°, respectively. It is important to note that these excited-state geometries are simply the lowest energy conformations of the molecules, and the TOP and TOQ dyes are likely to rotate about the heterocycle−phenyl linker in

Table 5. ωB97 S_1 Geometries of TOP Dyes

	1 (Å)[a]	2 (Å)[a]	3 (Å)[a]	α (°)[a]
TOP(DFT)	1.365	1.399	1.371	6.4
TOP_2(DFT)[b]	1.375	1.372	1.327	25.9
TOQ(DFT)	1.374	1.393	1.343	3.0
TOQ_2(DFT)[b]	1.402	1.372	1.326	18.1

[a]See Figure 2. [b]Data reported for TOP_2 and TOQ_2 are the average for both heterocycle moieties.

solution. Fortunately, ring rotation does not appear to significantly alter the nature of the electronic transitions (Figures 4 and 6), which suggests that the primary impact of the ring rotation is expected to be a diminished Stokes shift at elevated temperatures and decreased viscosities.

In all cases, the length of the heterocycle−phenyl bond decreases in the S_1 excited state. This can be understood in terms of the zwitterionic character of the S_1 excited state; the opposite charges on the heterocycle and phenyl moieties strengthen the linker bond. Other spectroscopically invalidated functionals yield alternative S_1 excited-state geometries (Figures S26−S30 and Tables S6−S10). Overall, the ωB97 functional predicts that these four triazole dyes undergo significant excited-state structural relaxation, which is consistent with their "mega" Stokes shifts.

Just as the relative orientation of the conjugated rings could be rationalized using Hückel's rule, the relative orientations of these rings in the excited state are consistent with Baird's rule. Baird's rule is perhaps less appreciated than Hückel's rule, and it states that conjugated π systems with $4n$ electrons are aromatic in their first excited state, whereas conjugated π systems with $4n + 2$ electrons are anti-aromatic.[23] This is the opposite of Hückel's rule. The triazolopyridinium heterocycle, the triazoloquinolinium heterocycle, and the phenyl ring all have $4n + 2$ π electrons. This suggests that each of these moieties is aromatic in the S_0 ground state and anti-aromatic in the S_1 excited state. However, by rotating the phenyl ring into a coplanar arrangement with either the triazolopyridinium or triazoloquinolinium heterocycle, $4n$ π electron systems can be formed. These structural arrangements are likely aromatic, and hence favorable, in the S_1 excited state. Thus, the relative orientations of the heterocycle and phenyl moieties in TOP and TOQ dyes can be rationalized using Baird and Hückel's rules.

DISCUSSION

TOP and TOQ Photophysics. The computational data presented in this article provide detailed insight into the excitation transitions for TOP and TOQ dyes, which are generally consistent with previous reports. To make excitation transition band assignments for TOP and TOQ dyes, the TDDFT-predicted UV/Vis Abs spectra were generated using six different density functionals. The accuracies of the computational models were assessed by comparing experimental and computed Abs intensities, not transition energies, because UV/Vis Abs intensities depend upon the overlap of the donor and acceptor states. The TOP and TOP_2 excitation transitions had previously been assigned to charge transfer and $\pi \rightarrow \pi^*$ transitions, respectively,[3] based upon PBE density functional models,[27] and the BLYP models presented here are consistent with those assignments (Figure 8).[25,26] Similarly, the TOQ excitation transition had been previously assigned to a charge transfer transition based upon semi-empirical

https://doi.org/10.1021/acs.jpcb.2c04397
J. Phys. Chem. B 2022, 126, 6997−7005

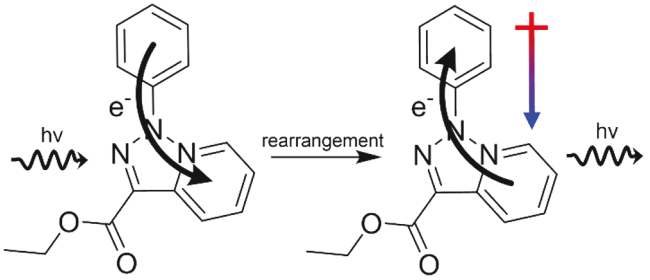

Figure 8. Proposed fluorescence mechanism for TOP. Light absorption by TOP induces intramolecular electron transfer from the phenyl ring to the heterocyclic ring, resulting in an excited state with zwitterionic character. Following excited-state structural relaxation, electron transfer back to the phenyl ring quenches the zwitterionic character and triggers the release of a photon.

calculations,[7] and that assignment is also supported by the BLYP model presented here. To our knowledge, the TOQ_2 excitation spectrum had not been modeled prior to this work. The spectroscopically validated BLYP model suggests a $\pi \rightarrow \pi^*$ assignment similar to TOP_2. Thus, this work corroborates prior assignments for the excitation transitions of TOP, TOP_2, and TOQ and provides the first validated band assignment for TOQ_2.

The computational data presented in this article yield the first validated band assignments for the fluorescence transitions of TOP and TOQ dyes. The S_1 excited-state structure and fluorescence spectrum for all four TOP and TOQ dyes were modeled using six different density functionals; a comparison of the predicted Stokes shifts to the experimental Stokes shifts revealed that the ωB97 range-separated functional provides the most accurate descriptions of the S_1 excited states (Table 4). The conclusion that two different density functionals, BLYP and ωB97, yield the most accurate descriptions of two different electronic states, S_0 and S_1, is not necessarily surprising. The magnitude of charge separation in the S_1 excited state is significantly greater than in the S_0 ground state, and the range-separated functionals were designed to provide improved treatment of long-range electron exchange, resulting in better descriptions for charge transfer excited states.[30] Based upon the spectroscopically validated S_1 excited-state models (Figure 8), the fluorescence transition for three of the four dyes studied here (TOP, TOQ, and TOP_2) is essentially the inverse of the excitation transition with minor perturbations due to excited-state structural relaxation. However, the excitation and emission transitions for TOQ_2 are fundamentally different from one another. Following excitation, S_1 excited-state relaxation of TOQ_2 results in charge separation to form a zwitterionic excited state. Consequently, only TOP_2 maintains a delocalized excited state following excited-state relaxation.

Origin of the Stokes Shift. The computational data presented here provide the first detailed insight into the origin of the "giga" Stokes shift in TOP. At room temperature, the S_1 excited states of TOP and TOQ dyes are fluorescent with lifetimes of ~1 ns,[7] which precludes structural characterization. Thus, TDDFT excited-state optimizations were employed to generate excited-state structural models whose accuracies were evaluated on the basis of the predicted Stokes shifts (Table 4). The most readily apparent structural change in the S_1 excited state is a rotation along the heterocycle−phenyl bond from a ground-state conformation that is best described as twisted to an excited-state conformation that is best described as coplanar (Figure 9), the reverse of TICT![19] It is noteworthy that TOP and TOQ have both the largest ring rotations (60.3° and

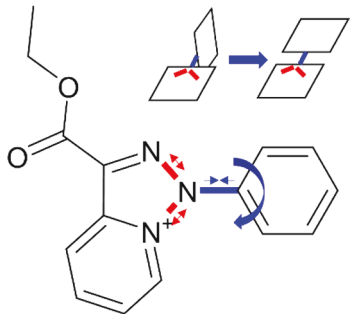

Figure 9. Prominent structural changes observed following photoexcitation of TOP. In accordance with Baird's rule, the phenyl and heterocycle rings adopt a coplanar orientation with a compressed C−N bond following excited-state relaxation (blue). In addition, the N−N bonds of the triazole moiety expand in the excited state due to the charge transfer nature of the excitation transition (red).

48.0°, respectively, Tables 1 and 5) and the largest Stokes shifts (11,200 and 9200 cm^{-1}, respectively). As noted above, these structural changes can be rationalized within the frameworks of Hückel and Baird's rules.[20−23] A twisted conformation may be favored in the S_0 ground state to yield two separate aromatic systems, and a coplanar conformation may be favored in the S_1 excited state to produce a single, delocalized aromatic system. It is interesting to note that a similar excited-state relaxation was recently proposed for other donor−acceptor fluorophores,[39−41] albeit for chromophores that do not exhibit a "giga" Stokes shift. These observations suggest that construction of a chromophore with two aromatic moieties separated by a single, rotatable bond may be a viable strategy for the development of novel fluorophores with "giga" Stokes shifts.

What are less apparent from inspection of the excited-state structures, but likely more significant with regard to the Stokes shift, are the structural changes within the triazole moiety upon photoexcitation. For all four TOP and TOQ dyes modeled here, the C−N bond between the heterocycle and phenyl groups shortens by nearly 0.1 Å (Figure 9). This bond shortening makes sense within the context of Baird's rule;[23] conjugation between the heterocycle and phenyl groups in the excited state will increase the double bond character of this bond. For TOP and TOQ, photoexcitation also lengthens the N−N bonds within the triazole by nearly 0.05 Å. This can be ascribed to the charge transfer transition populating a π^* orbital of this moiety. Although these bond length changes may seem small compared to the ring rotation upon photoexcitation, they are likely the major contributor to the Stokes shift. This is because bond stretches for aromatic systems are on the order of 2000−3000 cm^{-1} and, as a result, small structural changes have large energetic consequences. The N−N bond length changes are derived from the charge transfer nature of the photoexcitation, which suggests that the design of a "giga" Stokes shift chromophore from rotatable aromatic moieties could be further optimized by maximizing the charge transfer nature of the photoexcitation.

Photophysical Origins for "Giga" Stokes Shifts. This article has identified a second photophysical mechanism that yields "giga" Stokes shift fluorophores. As noted earlier, the majority of "giga" Stokes shift fluorophores reported to date

https://doi.org/10.1021/acs.jpcb.2c04397
J. Phys. Chem. B 2022, 126, 6997−7005

arise from TICT.[4−6] There are two aspects of TICT that are primarily responsible for the "giga" Stokes shift of these fluorophores: excited-state structural relaxation from a planar conformation to a twisted conformation and solvent reorganization to accommodate a zwitterionic excited state.[19] To our knowledge, the TOP dyes are currently the sole examples of "giga" Stokes shift fluorophores that do not follow a TICT mechanism.[3,7] As such, these compounds represent a new lead for the development of novel "giga" Stokes shift fluorophores. It should be noted that the excited-state aromaticity reversal observed for TOP dyes has also been invoked in the past for excited-state proton transfer reactions.[42−44] In addition, aromaticity reversal in an electronic excited state has also been invoked to explain aggregation-induced emission and the fluorescence of macromolecular structures.[45,46] Clearly, the influence of Baird's rule on the photophysics of conjugated fluorophores is a topic that merits further study.

CONCLUSIONS

In summary, spectroscopically validated computational models for TOP and TOQ photophysics have been developed. These models reveal that the excitation transitions of TOP and TOQ are best described as charge transfer, whereas the excitation transitions of TOP_2 and TOQ_2 are better described as $\pi \rightarrow \pi^*$. The emission transitions of TOP, TOP_2, and TOQ are essentially the inverse of their excitation transitions, with minor perturbations due to structural relaxation in the excited state. However, charge localization in the excited state of TOQ_2 results in an emission transition that is best described as charge transfer. This approach has yielded the first detailed models for the excited-state structures of TOP and TOQ. Inspection of these structures reveals that the "giga" Stokes shift of TOP arises from ring rotation and triazole bond weakening in the excited state. These observations suggest that novel "giga" Stokes shift fluorophores could be designed by focusing on two features: a pair of conjugated moieties that have different relative orientations according to Hückel and Bairds' rules and maximizing charge transfer between these two moieties upon photoexcitation.

ASSOCIATED CONTENT

Supporting Information

The Supporting Information is available free of charge at https://pubs.acs.org/doi/10.1021/acs.jpcb.2c04397.

S_0 and S_1 geometries, TDDFT-predicted UV/Vis Abs and fluorescence spectra, and Cartesian coordinates for all computational models (PDF)

AUTHOR INFORMATION

Corresponding Author

Matthew D. Liptak − *Department of Chemistry, University of Vermont, Burlington, Vermont 05405, United States;* orcid.org/0000-0002-4951-6636; Email: matthew.liptak@uvm.edu

Authors

Adam N. Petrucci − *Department of Chemistry, University of Vermont, Burlington, Vermont 05405, United States*

Morgan E. Cousins − *Department of Chemistry, University of Vermont, Burlington, Vermont 05405, United States*

Complete contact information is available at: https://pubs.acs.org/10.1021/acs.jpcb.2c04397

Funding

M.D.L. thanks the National Science Foundation (DMR-1506248) for financial support.

Notes

The authors declare no competing financial interest.

ACKNOWLEDGMENTS

The authors acknowledge Ivan Aprahamian (Dartmouth College) for helpful discussions and a critical reading of the manuscript.

REFERENCES

(1) Nagy, K.; Orbán, E.; Bősze, S.; Kele, P. Clickable long-wave "mega-Stokes" fluorophores for orthogonal chemoselective labeling of cells. *Chem. − Asian J.* **2010**, *5*, 773−777.

(2) Mohd Yusof Chan, N. N.; Idris, A.; Zainal Abidin, Z. H.; Tajuddin, H. A.; Abdullah, Z. White light employing luminescent engineered large (mega) Stokes shift molecules: a review. *RSC Adv.* **2021**, *11*, 13409−13445.

(3) Su, X.; Liptak, M. D.; Aprahamian, I. Water soluble triazolopyridiniums as tunable blue light emitters. *Chem. Commun.* **2013**, *49*, 4160−4162.

(4) Cao, C.; Liu, X.; Qiao, Q.; Zhao, M.; Yin, W.; Mao, D.; Zhang, H.; Xu, Z. A twisted-intramolecular-charge-transfer (TICT) based ratiometric fluorescent thermometer with a mega-Stokes shift and a positive temperature coefficient. *Chem. Commun.* **2014**, *50*, 15811−15814.

(5) Shaya, J.; Fontaine-Vive, F.; Michel, B. Y.; Burger, A. Rational design of push-pull fluorene dyes: synthesis and structure-photophysics relationship. *Chem. − Eur. J.* **2016**, *22*, 10627−10637.

(6) Arivazhagan, C.; Maity, A.; Bakthavachalam, K.; Jana, A.; Panigrahi, S. K.; Suresh, E.; Das, A.; Ghosh, S. Phenothiazinyl boranes: a new class of AIE luminogens with mega Stokes shift, mechanochromism, and mechanoluminescence. *Chem. − Eur. J.* **2017**, *23*, 7046−7051.

(7) Carboni, V.; Su, X.; Qian, H.; Aprahamian, I.; Credi, A. Blue-light-emitting triazolopyridinium and triazoloquinolinium salts. *ChemPhotoChem* **2017**, *1*, 222−229.

(8) Martin, A.; Moriarty, R. D.; Long, C.; Forster, R. J.; Keyes, T. E. Napthyridyl-substituted 4,4-difluoro-4-bora-3a,4a-diaza-*s*-indacene (BODIPY) luminophores: photophysis and application as molecular imaging probes in live cells. *Asian J. Org. Chem.* **2013**, *2*, 763−778.

(9) Moriarty, R. D.; Martin, A.; Adamson, K.; O'Reilly, E.; Mollard, P.; Forster, R. J.; Keyes, T. E. The application of water soluble, mega-Stokes-shifted BODIPY fluorophores to cell and tissue imaging. *J. Microsc.* **2014**, *253*, 204−218.

(10) O'Connor, D.; Byrne, A.; Berselli, G. B.; Long, C.; Keyes, T. E. Mega-stokes pyrene ceramide conjugates for STED imaging of lipid droplets in live cells. *Analyst* **2019**, *144*, 1608−1621.

(11) Más-Montoya, M.; Montenegro, M. F.; Espinosa Ferao, A.; Tárraga, A.; Rodríguez-López, J. N.; Curiel, D. Rigid π-extended boron difluoride complex with mega-Stokes shift for bioimaging. *Org. Lett.* **2020**, *22*, 3356−3360.

(12) Tang, F.; Liu, J.-Y.; Wu, C.-Y.; Liang, Y.-X.; Lu, Z.-L.; Ding, A.-X.; Xu, M.-D. Two-photon near-infrared AIE luminogens as multifunctional gene carriers for cancer theranostics. *ACS Appl. Mater. Interfaces* **2021**, *13*, 23384−23395.

(13) Wangngae, S.; Chansaenpak, K.; Nootem, J.; Ngivprom, U.; Aryamueang, S.; Lai, R.-Y.; Kamkaew, A. Photophysical study and biological applications of synthetic chalcone-based fluorescent dyes. *Molecules* **2021**, *26*, 2979.

(14) Gupta, S.; Milton, M. D. Novel Y-shaped AIEE-TICT active π-extended quinoxalines-based donor-acceptor molecules displaying acidofluorochromism and temperature dependent emission. *J. Photochem. Photobiol., A* **2022**, *424*, 113630.

(15) Boonkitpatarakul, K.; Wang, J.; Niamnont, N.; Liu, B.; Mcdonald, L.; Pang, Y.; Sukwattanasinitt, M. Novel turn-on fluorescent sensors with mega Stokes shifts for dual detection of Al^{3+} and Zn^{2+}. *ACS Sens.* **2016**, *1*, 144−150.
(16) Jarutikorn, S.; Kraithong, S.; Sirirak, J.; Panchan, W.; Sooksimuang, T.; Charoenpanich, A.; Wanichacheva, N. Environmentally friendly Ag^{+} detection of "turn-on" fluorescent sensor with a mega-Stokes shift and its application in biological systems. *Orient. J. Chem.* **2019**, *35*, 1227−1234.
(17) Gunturkun, D.; Isci, R.; Sütay, B.; Majewski, L. A.; Faraji, S.; Ozturk, T. Copolymers of 3-arylthieno[3,2-*b*]thiophenes bearing different substituents: synthesis, electronic, optical, sensor and memory properties. *Eur. Polym. J.* **2022**, *170*, 111167.
(18) Isci, R.; Varzeghani, A. R.; Kaya, K.; Sütay, B.; Tekin, E.; Ozturk, T. Triphenylamine/tetraphenylethylene substituted 4-thieno-[3,2-*b*]thiophen-3-ylbenzonitriles: synthesis, photophysical-electronic properties, and applications. *ACS Sustainable Chem. Eng.* **2022**, *10*, 1605−1615.
(19) Grabowski, Z. R.; Rotkiewicz, K.; Rettig, W. Structural changes accompanying intramolecular electron transfer: focus on twisted intramolecular charge-transfer states and structures. *Chem. Rev.* **2003**, *103*, 3899−4032.
(20) Hückel, E. Quantentheoretische Beiträge zum Benzolproblem I. Die Elektronenkonfiguration des Benzols und verwandter Verbindungen. *Z. Phys.* **1931**, *70*, 204−286.
(21) Hückel, E. Quantentheoretische Beiträge zum Benzolproblem II. Quntentheorie der induzierten Polaritäten. *Z. Phys.* **1931**, *72*, 310−337.
(22) Hückel, E. Quantentheoretische Beiträge zum Problem der aromatischen und ungesättigten Verbindunger. III. *Z. Phys.* **1932**, *76*, 628−648.
(23) Baird, N. C. Quantum organic photochemistry. II. Resonance and Aromaticity in the lowest $^{3}\pi\pi^{*}$ state of cyclic hydrocarbons. *J. Am. Chem. Soc.* **1972**, *94*, 4941−4948.
(24) Neese, F. Software update: the ORCA program system, version 4.0. *Wiley Interdiscip. Rev.: Comput. Mol. Sci.* **2011**, *8*, No. e1327.
(25) Becke, A. D. Density-functional exchange-energy approximation with correct asymptotic behavior. *Phys. Rev. A* **1988**, *38*, 3098−3100.
(26) Lee, C.; Yang, W.; Parr, R. G. Development of the Colle-Salvetti correlation-energy formula into a functional of the electron density. *Phys. Rev. B* **1988**, *37*, 785−789.
(27) Perdew, J. P.; Burke, K.; Ernzerhof, M. Generalized gradient approximation made simple. *Phys. Rev. Lett.* **1996**, *77*, 3865−3868.
(28) Becke, A. D. Density-functional thermochemistry. III. The role of exact exchange. *J. Chem. Phys.* **1993**, *98*, 5648−5652.
(29) Perdew, J. P.; Ernzerhof, M.; Burke, K. Rationale for mixing exact exchange with density functional approximations. *J. Chem. Phys.* **1996**, *105*, 9982−9985.
(30) Chai, J.-D.; Head-Gordon, M. Systematic optimization of long-range corrected hybrid-density functionals. *J. Chem. Phys.* **2008**, *128*, No. 084106.
(31) Weigend, F.; Ahlrichs, R. Balanced basis sets of split valence, triple valence and quadruple valence quality for H to Rn: design and assessment of accuracy. *Phys. Chem. Chem. Phys.* **2005**, *7*, 3297−3305.
(32) Weigend, F. Accurate Coulomb-fitting basis sets for H to Rn. *Phys. Chem. Chem. Phys.* **2006**, *8*, 1057−1065.
(33) Izsák, R.; Neese, F. An overlap fitted chain of speheres exchange method. *J. Chem. Phys.* **2011**, *135*, 144105.
(34) Barone, V.; Cossi, M. Quantum calculation of molecular energies and energy gradients in solution by a conductor solvent model. *J. Phys. Chem. A* **1998**, *102*, 1995−2001.
(35) Laaksonen, L. A graphics program for the analysis and display of molecular dynamics trajectories. *J. Mol. Graphics* **1992**, *10*, 33−34.
(36) Bergman, D. L.; Laaksonen, L.; Laaksonen, A. Visualization of solvation structures in liquid mixtures. *J. Mol. Graphics Modell.* **1997**, *15*, 301−306.
(37) Jacquemin, D.; Wathelet, V.; Perpète, E. A.; Adamo, C. Extensive TD-DFT Benchmark: Singlet-excited states of organic molecules. *J. Chem. Theory Comput.* **2009**, *5*, 2420−2435.
(38) Kasha, M. Characterization of electronic transitions in complex molecules. *Discuss. Faraday Soc.* **1950**, *9*, 14−19.
(39) Sissa, C.; Painelli, A.; Terenziani, F.; Trotta, M.; Ragni, R. About the origin of the large Stokes shift in aminoalkyl substituted heptamethine cyanine dyes. *Phys. Chem. Chem. Phys.* **2020**, *22*, 129−135.
(40) Ahmed, R.; Manna, A. K. Origins of large Stokes shifts in a pyrene-styrene-based push-pull organic molecular dyad in polar solvents and large electron mobility in the crystalline state: a theoretical perspective. *J. Phys. Chem. C* **2022**, *126*, 423−433.
(41) Ahmed, R.; Manna, A. K. Understanding high fluorescence quantum yield and simultaneous large Stokes shift in phenyl bridged donor-π-acceptor dyads with varied bridge lengths in polar solvents. *J. Phys. Chem. A* **2022**, *126*, 4221−4229.
(42) Lampkin, B. J.; Nguyen, Y. H.; Karadakov, P. B.; VanVeller, B. Demonstration of Baird's rule complementarity in the singlet state with implications for excited-state intramolecular proton transfer. *Phys. Chem. Chem. Phys.* **2019**, *21*, 11608−11614.
(43) Wu, C.-H.; Karas, L. J.; Ottosson, H.; Wu, J. I.-C. Excited-state proton transfer relieves antiaromaticity in molecules. *Proc. Natl. Acad. Sci.* **2019**, *116*, 20303−20308.
(44) Su, S.; Liang, X.; Fang, H. The effect of ring aromaticity on ESIPT behavior and photophysical properties of 2-(2′-hydroxyphenyl)-4-chloromethylthiazole derivatives: a TD-DFT study. *J. Mol. Liq.* **2021**, *334*, 116517.
(45) Zhao, Z.; Zheng, X.; Du, L.; Xiong, Y.; He, W.; Gao, X.; Li, C.; Liu, Y.; Xu, B.; Zhang, J.; Song, F.; Yu, Y.; Zhao, X.; Cai, Y.; He, X.; Kwok, R. T. K.; Lam, J. W. Y.; Huang, X.; Phillips, D. L.; Wang, H.; Tang, B. Z. Non-aromatic annulene-based aggregation-induced emission system via aromaticity reversal process. *Nat. Commun.* **2019**, *10*, 2952.
(46) Peeks, M. D.; Gong, J. Q.; McLoughlin, K.; Kobatake, T.; Haver, R.; Herz, L. M.; Anderson, H. L. Aromaticity and antiaromaticity in the excited states of porphyrin nanorings. *J. Phys. Chem. Lett.* **2019**, *10*, 2017−2022.

https://doi.org/10.1021/acs.jpcb.2c04397
J. Phys. Chem. B 2022, 126, 6997−7005